

Energy-Efficient Baseband Function Deployments for Service-Oriented Open RAN

Haiyuan Li¹, Amin Emami¹, Karcus Assis², Antonis Vefas¹, Ruizhi Yang¹
Reza Nejabati¹, Shuangyi Yan¹, and Dimitra Simeonidou¹

Abstract—Recently open radio access network (Open RAN), which splits baseband functions into multiple process units at different locations has received considerable attentions from both industries and academia with the potential to enable a fully disaggregated RAN with more flexibility in delivering energy-saving and latency-sensitive applications. However, the significant increases of resource usage dynamics in both geographical and time and network complexity may lead to unnecessary high energy consumption in RANs without an efficient RAN function management policy. Many studies have proposed baseband function management solutions, however, the activation cost and data network resources of edge computing capacities have not been evaluated in much detail, as far as the authors know. In this paper, with the objective of minimizing energy consumption, meanwhile, satisfying the requests over the network under the constraints of latency and resource capacity, we propose a completed mixed integer linear programming (MILP) formulation, a multi-agent deep reinforcement learning-based algorithm and a heuristic (DCUH), to take user plane functions (UPFs) on the multi-access edge computing servers (MECs) and the activation consumption of MECs into consideration. Moreover, we prototype an OpenDaylight, OpenStack and Open Source Management and Orchestration-based Open RAN testbed to verify the feasibility of the proposed solutions. Results show the importance of hibernating the MEC after a certain time of network vacancy. DRL-based algorithm and DCUH can approach a similar performance as the benchmark of MILP and save more than 40% energy consumption compared to the first-fit algorithm. This study offers an important insight into the design of baseband deployment policies that greatly enhance user experience with better service and save Open RAN operational energy costs.

Index Terms—Energy-efficient, Open RAN, resource optimization, baseband function deployment, 5G and beyond

I. INTRODUCTION

RECENT advances in fifth-generation (5G) mobile networks require a more flexible radio access network (RAN) to deliver better services for diverse use cases, including ultra-reliable low latency communication (uRLLC), enhanced mobile broadband (eMBB) and massive machine type communications (mMTC) [1]–[3]. For its part, Open RAN, the latest industry-wide initiative, opens up the disaggregated RAN components and has drawn much attention

from researchers and industries, with the potential to allow operators to deploy RAN more flexibly to tailor service function chains (SFCs) and network slices. The baseband function is split into radio unit (RU), distributed unit (DU) and centralized unit (CU) with different options [4]. Network function virtualization allows flexible deployments of these RAN functions on any computing servers, such as RAN clusters or multi-access edge computing servers (MECs), with dynamic individual up/down scaling according to traffic requests [5]–[7]. Consequently, the connection between RU and user plane function (UPF) is divided into fronthaul, midhaul and backhaul. Despite the clear advantages of Open RAN and MEC, however, without an efficient baseband function management strategy, the inevitable human-caused resource usage dynamics in both space and time [8]–[10] and the increased network complexity with disaggregated modules may cause severe energy waste and operating costs in maintaining idle or unnecessary servers.

Many research efforts have been made in the designing of baseband function management strategies. Regarding the baseband unit (BBU) placement of centralized-RAN (C-RAN), by means of mixed integer linear programming (MILP), Tinini, *et al.* studied the most energy-efficient way to manage the placement of BBU to accommodate demands on the nodes of the network [11]. Similarly, Mijumbi, *et al.* implemented a multi-objective optimization problem that considered more practical constraints, such as latency and server capacity [12]. One major drawback of MILP, however, is its intractable complexity which hinders its application in practical networks. Alternatively, Gao, *et al.* proposed a DRL-based solution with offline execution advantage that decreases the reasoning delay. The minimization objectives include bandwidth usage, transport latency and the number of activated MECs that host BBU functions [13]. Despite approaching the performance of MILP in a small-scale network, retraining costs with continuous network changes and the exponential growth in action space in large scale networks with a significant number of nodes and links still remain unclear. In contrast, to reduce the number of required BBUs while maintaining the scalability, Sigwele, *et al.* proposed a simulated annealing and a genetic algorithm under the constraints of service coverage and quality of service (QoS) [14]. Nevertheless, the routing costs and the latency hard limitation were out of their consideration.

Although extensive studies have been carried out on designing of BBU placement solutions to reduce power costs in RANs, with the latest advance including enhanced common public radio interface (e-CPRI) and flexible ethernet technologies, fronthaul bandwidth and transmission delay have been

Haiyuan Li, Amin Emami, Antonis Vefas, Ruizhi Yang, Reza Nejabati, Shuangyi Yan and Dimitra Simeonidou are with the High Performance Networks Group, Smart Internet Lab, School of Computer Science, Electrical and Electronic Engineering, and Engineering Maths (SCEEM), Faculty of Engineering, University of Bristol¹, BS8 1QU, U.K. (e-mail: ocean.h.li.2018@bristol.ac.uk).

Karcus Day R. Assis is with the Electrical and Computer Engineering Department, Federal University of Bahia (UFBA)², Salvador-BA, Brazil and also as a visitor at University of Bristol¹, U.K.

Manuscript received XXXX YY, ZZZZ; revised YYYYYY XX, ZZZZ.

greatly reduced [15], [16], which allows further splitting of RAN functions. The two-tier architecture of centralized RAN is further evolved to three-tier Open RAN deployed in practice [17]. Open RAN brings a higher plasticity for operators in dealing with NG diverse requests although it is realized at the expense of network complexity in terms of the coexistence of X-Haul (fronthaul, midhaul and backhaul) traffic, multiple baseband functions, various latency tolerances, and so on.

To further accommodate heterogeneous requests in next generation (NG) RAN, similar to [13], Xiao, *et al.* designed a DRL-based baseband function placement and routing strategy, where the DRL action was changed from the selection of BBU to DU and CU. This method only handles one request in each reasoning step and is unable to deal with the competition between requests on the network resources [18]. In contrast, under the constraint of latency and network resources, Zorello, *et al.* and Xiao, *et al.* proposed MILPs and heuristics that can determine the SFCs for all requests while minimizing the power consumption of the network [19], [20]. Nevertheless, they ignored the gradual decrease in the size of traffic on the function chain, which may lead to misjudgment of resource exhaustion while the bandwidth is still sufficient. Moreover, most previous studies applied power rather than energy to evaluate the performance of their algorithm, and no studies have been reported about the energy and cost comparison between activating MECs and leaving them on standby [11], [14], [19], [20]. Last but not least, as user plane services are delegated to MECs in NG RAN, UPF, edge processing units (PU) and other core network functions are no longer limited to data center facilities but can also be deployed at network edges.

Collectively, previous studies acknowledge the critical role of management of baseband function placement in Open RAN. However, few studies have been reported with consideration of the UPF accessibility, the activation time and power footprint of MECs, as far as the authors are aware. In this paper, to minimize the energy consumption in a resource-constrained RAN, we prototype an Open RAN testbed and propose three algorithms to manage the activation of MECs, deployment of DU, CU and UPF and provisioning of routing paths that go through tightly-intertwined SFCs. In contrast to existing works, we consider UPF on MEC and activation costs and verify the feasibility of the proposed solutions on a small-scale field-trial testbed. The main contributions of this paper are as follows:

- Three solutions including a MILP formulation, a multi-agent DRL algorithm and a DU/CU/UPF deployment heuristic (DCUH) that jointly optimize MEC activation, function deployment and routing provisioning are designed to minimize network energy consumption under the constraints of diverse traffic requirements and network carrying capabilities.
- We build an OpenDaylight [21], OpenStack [22] and Open Source Management and orchestration based (OSM) [23] programmable Open RAN testbed at Bristol with three distributed MEC servers and explore the implementation of our algorithms in practical networks.

To the best of our knowledge, this is the first time that multiple UPFs and the energy consumption of MEC activation

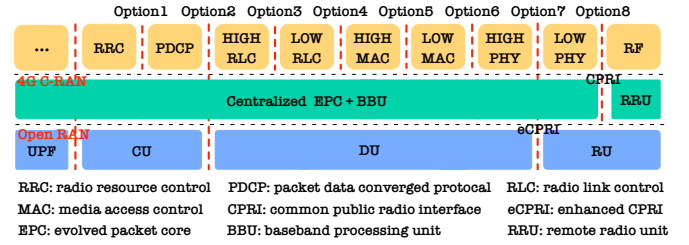


Fig. 1: Function Splitting Options of 4G C-RAN and Open RAN Proposed by 3GPP [24].

have been considered in the baseband function placement with feasibility verification in an Open RAN testbed. Simulation results show that it is profitless to hibernate a MEC when its vacant time is short. Baseband function deployment strategies that provide on-demand services only yield higher benefits than maintaining MECs on standby after a certain vacant time. Among the solutions examined in an 8-node network, DCUH and a DRL-based solution approach the optimal result of MILP with acceptable complexity, achieving more than 30%, 45% and 70% energy saving benefits compared to the random, first fit and all on standby strategies, respectively, with their performance maintained in large networks. Moreover, we detail the deployment of baseband functions on the testbed and verify these simulation results and the feasibility of algorithms by power monitoring of three different depths of server activation and a loading stress test.

The remainder of this paper is organized as follows. Section II introduces the concept of baseband function deployments in NG RAN. Section III and IV detail a MILP formulation and a multi-agent DRL algorithm. Another heuristic solution DCUH is presented in Section V. The simulation results are given in Section VI. Section VII details the implementation of our testbed at Bristol and reports the feasibility evaluation. Finally, Section VIII concludes the paper.

II. CONCEPT OF BASEBAND FUNCTION DEPLOYMENT

In the fourth-generation network, by leveraging cloud technologies, C-RAN consolidates baseband processing in centralized BBUs. The low-phy layer radio frequency (RF) functions are delivered by remote radio units (RRU) close to the antennas in large-scale scenarios. [25], [26]. C-RAN increases energy efficiency and resource utilization with denser RRU deployments and fewer active cell sites when requested. However, NG traffic requires a more flexible RAN architecture to accommodate higher fronthaul bandwidth and latency requirements. Relying on emerging edge computing and network function virtualization technologies, 3GPP and other standardization bodies proposed a new concept, Open RAN, that includes multiple baseband functions which are able to be virtualized and tailored in MEC networks in response to heterogeneous requests [27]–[29]. To demonstrate the difference between the two concepts, their function splitting options are summarized in Figure 1. Compared to C-RAN, there are different splitting options to separate baseband functions in Open RAN. In particular, functional split option 7 and option 2 between RU, DU and CU are selected in our experiment and testbed solution.

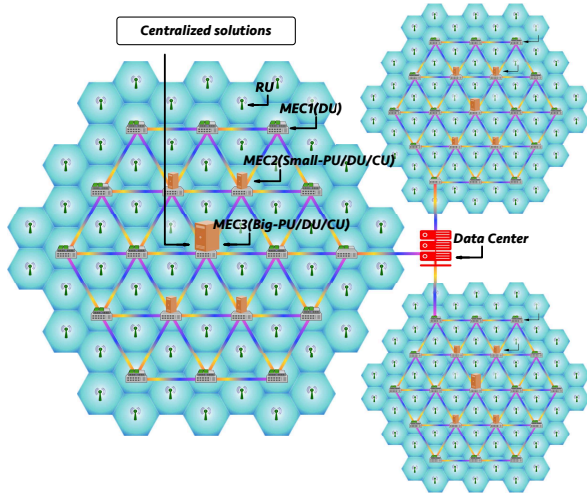


Fig. 2: Open RAN Cluster Model Composed of RU, MEC1, MEC2, MEC3 and DC.

To reduce the management complexity, we partition a large cellular network consisted of MECs into multiple clusters, where some of them share the same data center facility. The network architecture is shown in Figure 2. Within each cluster, an RU collects requests within its coverage area and sends them to proximate MECs through fibers. To acquire network service, each group of requests needs to go through a SFC consisting of DU, CU and UPF.

Since MECs have different types and amounts of hardware composition, we classified them into three categories, where MEC1 only provides DU service, MEC2 can be used as DU, CU and UPF, and MEC3 has the same functionalities as MEC2 but with more resources. Assuming the RAN network has limited computing resources on MECs, they stay either in activation or hibernation mode before requests arrive. Without proper resource management, computing resources will be wasted with unnecessary energy consumption. In dealing with the competition between requests, it is necessary to design a service-oriented strategy to jointly manage the working status of MECs, the deployment of baseband functions on activated servers and the provisioning of routing paths for the network function chains. A centralized solution can be placed on a MEC with a global view of requesting information and network resource status. It is worth mentioning that energy-saving features of the RAN network will be highly dependent on the cost of activating the MEC from its hibernation mode.

III. MILP FORMULATION FOR BASEBAND FUNCTION DEPLOYMENTS

Based on the concept of baseband function deployment, we formulate a MILP problem to jointly optimize the deployment of DU/CU/UPF and routing provisioning. Multi-function deployment and multi-latency limitations are the major novelties of the developed MILP with respect to previous studies. The formulation is resolved using IBM ILOG CPLEX solver. For ease of reference, important notations used throughout this paper are summarized in Table I.

TABLE I: Notations Used Throughout the Paper

	Notation	Description
Index	u	Activated MEC server
	s and d	Source and destination of a set of requests
	i and j	Origination and termination of a virtual link
	m and n	Endpoints of a physical link
	f	Network function
Given	N	MEC server set
	E	Link set
	$G = (N, E)$	Network graph representation
	B_w	Bandwidth of physical link.
	E_u	Activation energy of u
	E_w	Unified switching energy cost
	m_f	Maximum capability of f
	G_u^ϵ	DU capacity of u
	G_u^σ	CU capacity of u
	G_u^η	PU core capacity of u
	T^s	Traffic from the source s
	c_s	Computing resource requirement of s
	d_{mn}	Distance between m and n
	l_q^s	Acceptable fronthaul distance of s
	l_p^s	Acceptable end-to-end distance of s
	χ	An arbitrarily large number
	ϵ	An arbitrarily small number
	ψ	Traffic decreasing ratio after DU
	$\rho_k(f, g)$	Function ordering indicator. It is 1 (resp. -1) if f appears before (resp. after) g
	α_u^ϵ	Equals to 1 if u has activated DU; (binary)
	α_u^σ	Equals to 1 if u has activated CU; (binary)
	α_u^η	Equals to 1 if u has activated UPF; (binary)
	n_d^η	Requested computing cores on d
	v_{ij}^d	Virtual link arriving in d
	Λ^{sd}	Possible traffic flow from s to d .
	V_{ij}	Total aggregated traffic of a virtual link from i to j
	l_{ij}	Total distance of an established virtual link from i to j
	λ_{ij}^{sd}	The component of s - d node pair traffic offered onto a virtual link from i to j
	B_{ij}^{sd}	Equals to 1 if $\lambda_{ij}^{sd} > 0$; equals to 0 if $\lambda_{ij}^{sd} = 0$
	P_{mn}^{ij}	The traffic that a virtual link from i to j passes through in link m - n (integer).
	A_{mn}^{ij}	Used for defining virtual link routing on the physical topology. A_{mn}^{ij} is equal to 1 if $P_{mn}^{ij} > 0$; equal to 0 if $P_{mn}^{ij} = 0$ (binary)
	$b_{f,u}$	Number of f (DU or CU) located on node u (integer).
	$y_{f,u}^{sd}$	Equals to 1 if function f handles traffic sd on node u (binary).
	$Y_{f,u}^{sd}$	Equals to 1 if sd meets its assigned f either before or on node u (binary)
	S^{sd}	Number of nodes switching when traffic goes from s to d
	b^{sd}	It indicates if there is traffic from s to d (binary)

A. MILP formulation

The objective of this paper is to minimize the energy consumption in the network while satisfying all traffic requirements and resource limitations. Consistent with [19], [20], the energy consumption of the server is assumed to increase linearly according to the size and amounts of the requests. Therefore, the energy consumption of a specific task is independent to the function placement, and only determined by the size of the required computing resource. In addition, as some requests require edge computing service, we consider UPF and its connected PU as a whole to be located at the same MEC, and the requests received on a MEC belong to the

same network slice and share a common latency requirement. Among DU, CU and PU, they are all limited by bandwidth and computing resources. To simplify the problem, according to the degree to which the three modules are limited by resource types, we set DU and CU to be constrained by the access bandwidth in units of Gbits/s, and PU to be constrained by computing resources in units of cores.

Since network cost and energy consumption are determined by activated MECs and routing paths, Equation 1 represents the objective function, where E_u is the activation energy cost of MEC u . α_u^ϵ , α_u^σ , α_u^η are binary variables and denote the placement decisions of DU, CU and UPF on MEC u for requests received by MEC s . S^{sd} is the switching times of requests sd and E_u is the unified switching energy cost. Overall, the objective function can be interpreted as achieving optimal energy cost through two joint policies of placement and routing to minimize the number of activating MEC1/2/3s and switching times. Let λ_{ij}^{sd} be the traffic from sd pair on link ij and V_{ij} be the traffic on link ij from all sd pairs. Equation 2 stands for the flow conservation constraints on virtual layer, where Λ^{sd} is a variable working together with Equation 3 to attend the traffic from T^s . Equations 4 and 5 are total flow constraints on a virtual link, and Equation 5 is used as an indicator for virtual links with traffic sd . Therefore, Equations 6, 7 and 8 indicate the virtual links arriving at a destination node d from any node s and count the amount of them. Equation 9 represents the flow conservation constraints of routing at the physical layer. Equation 10 denotes that the utilized bandwidth should not exceed the bandwidth capacity of the physical link. Equation 11 indicates where virtual link ij passes on physical link mn . Equation 12 prevents traffic from being partitioned and Equations 13, 14 and 15 define the latency fronthaul and latency end-to-end constraints. Constraint 16 indicates that each function instantiation has a limited capacity and needs to be duplicated enough to handle the traffic that is assigned to it on the corresponding node. Constraints 17, 18 and 19 state that at the source, a commodity has met none of the functions, whereas at the destination, it has met all the functions included in its chain, respectively. Constraint 20 accounts for the order of the functions within the same chain: when a function g appears before f on the same SFC. (Therefore, $\rho_k(f, g) = -\rho_k(g, f) = -1$). Equation 21, 22 and 23 define the activation of UPF, DU and CU, respectively. Constraints 24 and 25 ensure that the distributed DU, CU from MEC u do not exceed its carrying capability, where ψ is the traffic decreasing ratio after process by DU. Because the traffic size decreases after DU, fronthaul bandwidth is considered individually. By subtracting from "1", Equation 26 counts the number of virtual links of sd pair and finds the number of switches that occurred from the s to d of this pair. Equation 27 indicates if there is traffic from s to d . Finally, Equation 28 limits the number of processing cores of PU. Overall, the optimization problem P is formulated as follows:

Objective:

$$\min \sum_{u,s,d} ([(\alpha_u^\epsilon + \alpha_u^\sigma + \alpha_u^\eta)/3] E_u + S^{sd} E_w) \quad (1)$$

Subject to:

$$\sum_j \lambda_{ij}^{sd} - \sum_j \lambda_{ji}^{sd} = \begin{cases} \Lambda^{sd} & i = s \\ -\Lambda^{sd} & i = d \\ 0 & i \neq s, d \end{cases} \quad (2)$$

$$\sum_d \Lambda^{sd} = T^s \quad \forall s \neq d \quad (3)$$

$$\lambda_{ij}^{sd} \leq \Lambda^{sd} \quad \forall s, d, i, j \quad (4)$$

$$\sum_{sd} \lambda_{ij}^{sd} = V_{ij} \quad \forall i, j \quad (5)$$

$$B_{ij}^{sd} = \lceil \frac{\lambda_{ij}^{sd}}{\chi} \rceil \quad \forall s, d, i, j \quad (6)$$

$$\sum_s B_{ij}^{sd} = v_{ij}^d \quad \forall s \neq d \quad (7)$$

$$\sum_{ij} v_{ij}^d = n_d^\eta \quad \forall d; \quad (8)$$

$$\sum_n P_{mn}^{ij} - \sum_n P_{nm}^{ij} = \begin{cases} V_{ij} & m = i \\ -V_{ij} & m = j \\ 0 & m \neq i, j \end{cases} \quad \forall i, j, m \quad (9)$$

$$\sum_{ij} P_{mn}^{ij} \leq B_w \quad \forall mn \quad (10)$$

$$A_{mn}^{ij} = \lceil \frac{P_{mn}^{ij}}{\chi} \rceil \quad \forall i, j, m, n \quad (11)$$

$$A_{mn}^{ij} + A_{ml}^{ij} \leq 1 \quad \forall i, j, m \quad n \neq l \quad (12)$$

$$\sum_{mn} A_{mn}^{ij} d_{mn} = l_{ij} \quad \forall i, j \quad (13)$$

$$\sum_{ij} B_{ij}^{sd} l_{ij} \leq l_q^s \quad \forall j = u, DU \in u \quad (14)$$

$$\sum_{ij} B_{ij}^{sd} l_{ij} \leq l_p^s \quad \forall s, d = u, UPF \in u \quad (15)$$

$$m_f b_{f,u} \geq \sum_{sd,i} y_{f,u}^{sd} \Lambda^{sd}, \quad \forall f, u \quad (16)$$

$$Y_{f,s}^{sd} = 0 \quad \forall s, d, f \quad (17)$$

$$Y_{f,d}^{sd} = 1 \quad \forall s, d, f \quad (18)$$

$$(B_{ij}^{sd} - 1) + Y_{f,j}^{sd} - Y_{f,i}^{sd} \leq y_{f,j}^{sd} \quad \forall s, d, i, j, f \quad (19)$$

$$Y_{f,j}^{sd} - Y_{g,i}^{sd} \geq \rho_k(f, g) \quad \forall s, d, i, j, f; \quad (20)$$

$$\alpha_d^\eta = \lceil \frac{n_d^\eta}{\chi} \rceil \quad \forall d \quad (21)$$

$$\alpha_u^\epsilon = \lceil \frac{b_{f,u}}{\chi} \rceil \quad \forall f = 1 = DU, \forall u \quad (22)$$

$$\alpha_u^\sigma = \lceil \frac{b_{f,u}}{\chi} \rceil \quad \forall f = 2 = CU, \forall u \quad (23)$$

$$\sum_{sd,i} \lambda_{iu}^{sd} \alpha_u^\epsilon \leq G_u^\epsilon \quad \forall u, DU \in u \quad (24)$$

$$\sum_{sd,i} \psi \lambda_{iu}^{sd} \alpha_u^\sigma \leq G_u^\sigma \quad \forall u, CU \in u \quad (25)$$

$$\sum_{ij} B_{ij}^{sd} - 1 = S^{sd} \quad \forall s, d \quad (26)$$

$$b^{sd} = \lceil \frac{\Lambda^{sd}}{\chi} \rceil \quad \forall s, d \quad (27)$$

$$\sum_s c_s b^{sd} \leq G_d^\eta \quad (28)$$

Our MILP formulation is inspired by [30], however, their scheme does not allow network function placement on source nodes. As an improvement to the program, to enable function placement on any server of the network, we attach an auxiliary node that cannot be activated by other servers and affect MILP performance because of its huge energy cost. A negligible latency is also configured from each auxiliary node to its adjacent original node, allowing the auxiliary one activates the original one.

B. Complexity Analysis of the MILP

Regarding the complexity of the problem, we show that the DU/CU/UPF placement and routing is a non-deterministic polynomial-time hardness (NP-hard) problem by a reduction from another model. Derived from the bin-packing problem, authors in [20] proved this property in the optimization of DU/CU deployment with the constraints of bandwidth, latency and computing resources. On the basis of that, in this paper, multiple UPFs, traffic decreasing on the SFC and some other hard limitations further complicate the problem. Because of the transitivity of NP-Hardness, P in our paper is also NP-hard. In addition, non-linear constraints (16), (14)-(15) and (24)-(25) make the network more complex. As they are formed by the multiplication of a binary variable and an integer, to linearize the problem, we replace them with other constraints [31] such as strategies for equations with $\lceil * \rceil$ and constraint 4.11 in [32].

IV. MULTI-AGENT DRL-BASED BASEBAND FUNCTION DEPLOYMENTS

As the numbers of N and E increase, the MILP formulation becomes intractable to be solved in polynomial time. We design an online multi-agent DRL-based algorithm to improve the reaction time and adapt to complex network architectures. With the action of the DRL algorithm that determines activated MECs, a restricted function deployment heuristic (RFDH) is then proposed as a combined solution to optimize baseband function placement and routing provisioning on these activated servers and generate the corresponding reward. To resolve the aforementioned problem, we first model network responses of the function management to requests as a Markov Decision Process (MDP) [33]. A multi-agent DRL algorithm is explored to solve this MDP and find the optimal network function deployment policies, avoiding action space explosion in DRL. In the defined MDP, the discounted reward R_t for a batch of tasks Y is defined as

$$R_t = \sum_{y=0}^Y \gamma^y r_{t+y} \quad (29)$$

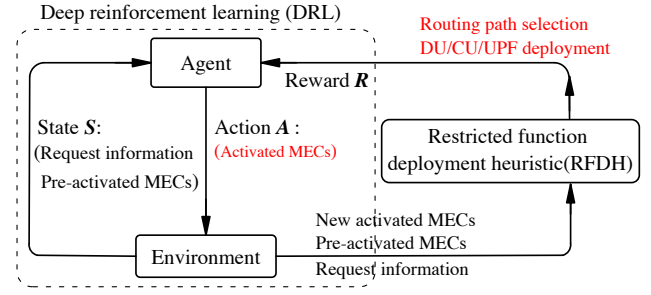


Fig. 3: Overall DRL-based Solution of Baseband Function Deployment (DRL: MEC activation strategy; RFDH: DU, CU, UPF deployment and routing strategy).

where γ is the discount factor that denotes the importance of following processing task rewards in Y and indirectly expresses the degree of correlation between each step. y is a natural number, and r_{t+y} is the reward of a certain task, $t+y$. Based on Equation 29, the action value function is defined to evaluate the action a_t by the discounted return at state s_t as follows:

$$Q_\pi(s_t, a_t) = \mathbb{E}[R_t | s_t, a_t] \quad (30)$$

π is the policy function and it represents the probability density function of the action. In addition, another critical component, the state value function, is also defined to demonstrate the expected discounted return for selecting state s_t as follows:

$$V_\pi(s_t) = \mathbb{E}[R_t | s_t] \quad (31)$$

where V_π can be used to assess the quality of the policy function π . The state value function can also be written as the expectation value of Q_π for action set A :

$$V_\pi(s_t) = \mathbb{E}_A[Q_\pi(s_t, A)] = \sum_a \pi(a | s_t) \cdot Q_\pi(s_t, a) \quad (32)$$

In general, the essence of our DRL solutions for MDP is to calculate the optimal value function and policy function, which are composed of the rewards of a batch of tasks. By achieving the maximum average reward of these requests, the DRL-based algorithm is able to acquire the optimal baseband function deployment policy for every individual DRL step, i.e. resolving the reward maximization problem formulated in Equation 1.

With the activated MECs determined by DRL, a heuristic RFDH is designed to deploy DU, CU and UPF on these activated MECs on the chosen routing paths. The detail of the RFDH is discussed in subsection IV-B. The overall DRL-based solution of baseband function deployment, i.e. the cooperation between DRL and RFDH is shown in Figure 3. The activation action done by DRL is used as input of RFDH. It decides the placement of baseband functions and then generates corresponding rewards for the training process. Two sections are geared together to resolve the optimization problem P .

A. Multi-agent deep deterministic policy gradient based MEC activation strategy

Multi-agent deep deterministic policy gradient (MADDPG) is used to solve the MDP. It is a promising DRL algorithm

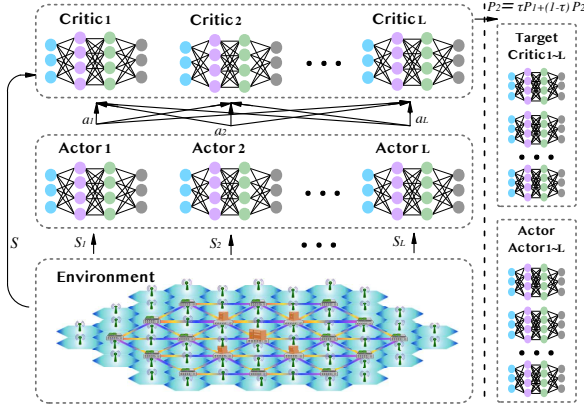


Fig. 4: Actor-Critic Architecture Used in Multi-agent Deep Deterministic Policy Gradient Solution.

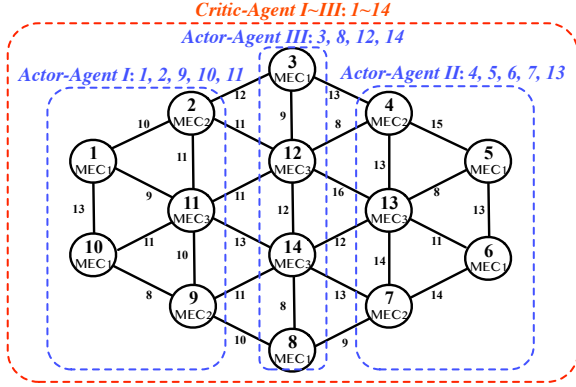


Fig. 5: Example of MADDPG Multi-agent Distribution for Baseband Function Deployment in a 14-MEC Network.

that uses policy gradient to estimate the maximum state value $V_\pi(s_t)$ [34]. Because the state value function is equal to the expectation value of Q_π as shown in Equation 32, the main idea of MADDPG is to get $V_\pi(s_t)$ by using two neural networks to approximate the policy function $\pi(a | s_t)$ and the action-value function $Q_\pi(s_t, a)$. The interaction between policy and action-value functions is realized by the actor-critic architecture [35]. Within this architecture, the actor neural network applies the policy gradient algorithm to optimize the policy function; the critic network uses the time differential (TD) algorithm [36] to estimate the corresponding action-value function. ‘Deterministic’ in MADDPG comes from the fact that the action output from the actor agent is a definite number instead of a probability distribution as in normal actor-critic architecture. This algorithm increases the scalability of DRL algorithms in large networks by dividing action space into smaller pieces.

In MADDPG, each agent needs a group of actor, target actor, critic and target critic neural networks. In this problem, we applied the same network state information to each actor. Then the actions decided by all actors are shared as input among each critic. The parameters of the target networks are updated from the corresponding actor and critic networks based on

$$P_2 = \tau P_1 + (1 - \tau) P_2 \quad (33)$$

where τ is the target network update coefficient. P_1 and P_2 are the parameter of evaluation networks and target networks,

Algorithm 1: Multi-agent Deep Deterministic Policy Gradient (MADDPG) Algorithm

- 1: Initialize replay memory \mathcal{B}
 - 2: Initialize the actor, target actor, critic and target critic with parameter $\theta_{1 \sim L}, \theta_{1 \sim L}^*, \omega_{1 \sim L}, \omega_{1 \sim L}^*$
 - 3: **for** n in batch **do**
 - 4: Initialize the network resource state
 - 5: Get state $s_{t, 1 \sim L}$
 - 6: Estimate $a_{t, 1 \sim L}$ by $\pi(s_{t, 1 \sim L}; \theta_{z, 1 \sim L})$
 - 7: Execute $a_{t, 1 \sim L}$, get reward $r_{t, 1 \sim L}$ and next state s_{t+1}
 - 8: Store $(s_{t, 1 \sim L}, a_{z, 1 \sim L}, r_{t, 1 \sim L}, s_{z+1, 1 \sim L})$ in \mathcal{B}
 - 9: Get minibatch from \mathcal{B}
 - 10: **for** m in minibatch **do**
 - 11: Estimate $a_{m+1, 1 \sim L}$ by $\pi(s_{m+1}; \theta_{m, 1 \sim L}^*)$
 - 12: Estimate $Q(s_{m, 1 \sim L}, a_{m, 1 \sim L} | \omega_{1 \sim L})$
 - 13: Estimate $Q(s_{m+1, 1 \sim L}, a_{m+1, 1 \sim L} | \omega_{1 \sim L}^*)$
 - 14: Use common reward for critics, $r_t = \bar{r}_{t, 1 \sim L}$
 - 15: Perform gradient descent for critic based on TD algorithm
 - 16: Get $d_{\omega, \theta, t} = \frac{\partial Q(s_{m+1}, \pi(s_{m+1}; \theta); \omega)}{\partial \theta} |_{\theta = \theta_{m, 1 \sim L}, \omega = \omega_{m, 1 \sim L}}$
 - 17: Perform gradient ascent for actor based on policy gradient algorithm:
 - 18: Update target network parameter based on
 - 19: $\theta_{1 \sim L}^* = \tau * \theta_{1 \sim L} + (1 - \tau) * \theta_{1 \sim L}^*$
 - 19: $\omega_{1 \sim L}^* = \tau * \omega_{1 \sim L} + (1 - \tau) * \omega_{1 \sim L}^*$
 - 20: **end for**
 - 20: **end for**
-

respectively [35]. It is designed to increase the converging speed. Overall, the multi agent actor-critic structure for our problem is shown in Figure 4.

In our solution, all servers in a cluster are assigned into L groups, corresponding to L DRL agents. The pre-activation status of N servers and the parameters for each request, including fronthaul delay l_q^s , end-to-end delay l_p^s , initial data size T_s and PU resource requirement c_s are shared between every actor and critic as state space components. On the basis of this state information, each actor is responsible for deciding which ones to activate in its assigned MECs. Therefore, within a N node network, the action space of each actor l is 2^{M_l} , and the state space size is $5 * N$. M_l is the number of MECs in the group L and $\sum_l M_l = N$. Based on the actor-critic architecture shown in Figure 4, we can acquire that the state space size of each critic is $L * 2^{M_l} + 5 * N$. In each critic, the output with shape $1 * 1$ is used as the criterion of the policy gradient algorithm for the corresponding actor. Taking a 14-node network shown in Figure 5 as an example, we can assign node 1, 2, 9, 10, 11 to actor agent I, node 4, 5, 6, 7, 13 to actor agent II and the rest to actor agent III. The action and state space of three actors are 32, 32, 16 and 70, 70, 70, respectively. Since the entire network information and actions done by three actors are input to three critics as state information, the state space of each critics is 150. With the increase in network size N , to realize the scalability, we can maintain an acceptable action space size 2^{M_l} with a larger number of agent L . As there is no partial observation between each actor, L agents can be placed on any server with vacant computing resources. Parallel computing technologies can be used to accelerate the training speed [37].

Algorithm 2: Restricted Function Deployment Heuristic

```

1: Store new activated and pre-activated MECs into list  $\mathcal{K}$ 
2: for all traffic  $s$ , MEC2/3  $u$  in  $\mathcal{K}$  do
3:   if  $s$  from  $u$  then
4:     Deploy UPF on  $u$  for  $s$ ,  $G_u^\eta - c_s$ 
5:   else
6:     Based on  $l_p^s$ , append  $s$  to ' $u$ ' in dictionary  $\mathcal{S}_0$ 
7:   end if
8: end for
9: Sort MEC2/3 in  $\mathcal{K}$ . The more requests a MEC can serve, the higher the ranking.
10: Sort requests in Values in  $\mathcal{S}_0$ . The more MECs a request can access, the more backward.
11: for MEC2/3  $u$  in  $\mathcal{K}$ , Sorted traffic  $s$  in  $\mathcal{S}_0[u']$  do
12:   if Rest  $G_u^\eta \geq c_s$  then
13:     Deploy UPF on  $u$  for  $s$ ,  $G_u^\eta - c_s$ 
14:   else
15:     DRL reward = -1
16:   end if
17: end for
18: Find paths from origins to corresponding destinations based on  $l_q^s$ , store into dictionary  $\mathcal{D}_0$ 
19: for activated MEC1/2/3  $u$  in  $\mathcal{K}$  do
20:   Deploy DU or CU for traffic  $s$  from  $u$ ,  $G_u^\epsilon - T_s$ ,  $G_u^\sigma - \psi T_s$ 
21: end for
22: for rest traffic  $s$  without DU do
23:   Based on  $l_q^s$  and  $\mathcal{D}_0$ , append acceptable MECs and paths from ' $s$ ' to destinations in dictionary  $\mathcal{S}_1$ 
24: end for
25: for Traffic  $s$  in Key list of  $\mathcal{S}_1$  do
26:   Sorting its paths based on the hops
27: end for
28: for rest traffic  $s$  in Key list of  $\mathcal{S}_1$  without DU do
29:   for all activated MEC1/2/3  $u$  in  $\mathcal{K}$  do
30:     for paths in  $\mathcal{S}_1[s']$  do
31:       if left  $G_u^\epsilon \geq T_s$  &
          bandwidth of each hop on the path before  $k \geq T_s$ 
          & bandwidth of each hop after DU  $\geq \psi T_s$  then
32:         Deploy DU on  $u$  for  $s$ ,  $G_u^\epsilon - T_s$ 
33:         Store the used paths into dictionary  $\mathcal{D}_1$ 
34:       else
35:         DRL reward = -1
36:       end if
37:     end for
38:   end for
39: end for
40: Deploy CU on Activated MECs in selected Paths
41: if left requests without CU then
42:   DRL reward = -1
43: else
44:   DRL reward =  $w_2/w_1$ 
45: end if

```

Fully cooperative (FC) method is adopted to minimize the activation energy consumption of the entire network. It means that L critics apply a common reward achieved by the interactions between all the actors and the DRL environment. The algorithms of MADDPG are demonstrated in the Algorithm 1. τ in the policy gradient algorithm is the coefficient to update the target network parameter. μ denotes the learning rate of DRL. θ , θ^* , ω and ω^* are parameters of actor, target actor, critic, and target critic, respectively.

B. Restricted function deployment heuristic (RFDH)

Restricted by the activation status decided by DRL, we propose a heuristic (RFDH) in Algorithm 2 that can firstly decide the baseband function deployment and routing paths and secondly calculate the reward and feed it back to the DRL agent. RFDH aggregates all activated MECs into a set \mathcal{K} . In order to obtain the corresponding rewards, except for the MECs in \mathcal{K} , other MECs are not allowed to be activated even if the resources are insufficient. During this process, UPF, DU and CU are deployed on the \mathcal{K} in turn according to latency and network capacity constraints. When distributing UPF and DU, RFDH sorts the accessible MECs in descending order by the number of requests they can serve. This is designed to satisfy the most requests with the least amount of resources. In addition, it also sorts the deployment decision priority of the requests in ascending order based on their selection space size. For instance, assuming in a network that nodes 5, 6 are pre-activated, and requests from nodes 1, 7, 8 are looking for UPF service. If 1, 7, 8 can get access to 5, 6, and 7, 8 can get access to 5, traffic from node 1 will have a higher priority than 7 and 8 to be serviced by 6 as it only has one choice. It ensures limited resources will not be wasted for inappropriate resource allocation. Regarding the path provisioning process, Depth-First Search (DFS) algorithm [38] is adopted to traverse all available paths subject to the end-to-end delay l_p^s . Within the optional routing space, subject to the bandwidth limitation, routing path provisioning is in accordance with the principle that the fewer hops, the higher the priority to reduce switching energy consumption.

Since the premise of DRL actions on activating MECs is to fulfill all requests even if it leads to higher energy consumption, the reward is set to -1 as punishment if there is any unserved request. Otherwise, it is equal to w_2/w_1 , where w_1 is the energy consumption determined by DRL for routing and activating MECs, and w_2 is the energy cost when all the servers are activated. Consistent with the objective function 1, this design provides greater rewards for actions that use less energy, thereby, minimizing energy consumption while satisfying all requests over the network.

The complexity of the RFDH is calculated as follows. Under the assumption of m activated MEC1s and J activated MEC2s and MEC3s, the complexity of distributing UPF services from activated MECs in \mathcal{K} is $O(2NJ + J\log J + N\log N - J^2)$, where Merge Sort [39] is used as the sorting algorithm. Based on the distributed MECs, we applied the DFT to find all the qualified paths with the time complexity of $O(N^2 + NE)$. After that, the complexity of utilizing $(J+m)$ activated MECs for DU and CU service can be represented by $O(2N + (N - J - m)S_1 \log S_1 + (N - J - m)(J + m)S_1)$, where S_1 is the average length of Values in dictionary \mathcal{S}_1 in Algorithm 2. Overall, the time complexity of RFDH can be written as $O(2NJ - J^2 + J\log J + N\log N + 2N + (N - J - m)S_1 \log S_1 + (N - J - m)(J + m)S_1)$.

V. BASEBAND FUNCTION DEPLOYMENT HEURISTIC

Despite MADDPG-based algorithm eliminating action space explosion in dealing with function placement problems,

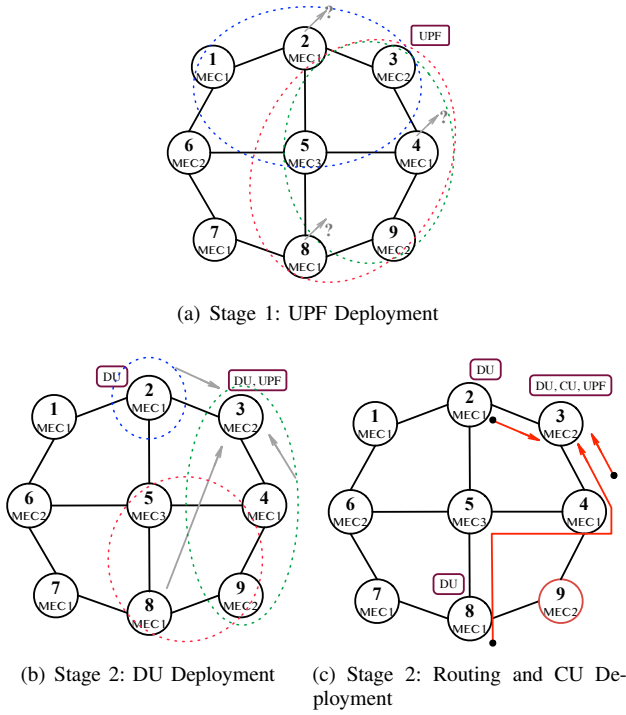


Fig. 6: DCUH Example; In (a) and (b), blue, green and red dash circles represent the farthest acceptable distance under end-to-end and fronthaul delay constraints of traffic from Node2, Node4 and Node8, respectively; In (c), red arrows represent the working paths.

the randomness of the states and the uncertainty of the cooperation between DRL agents may undermine the accuracy of prediction performance. Hence, in addition, we design a heuristic algorithm DCUH consisting of two stages as shown in Algorithm 3. First, it finds out the destination MECs for UPF deployment. Following the objective of P , DCUH selects the appropriate MECs for the deployment of the remaining baseband functions and routing paths. The two stages together with their strategies are described in the following subsections.

A. Heuristic Algorithm

In the first stage, facing the computing requirements raised by the requests, DCUH decides their corresponding UPFs according to the the end-to-end delay constraint and PU resource limitation of different MECs. On the basis of these deployed UPFs, in stage II, DCUH helps to find the DU, CU under the constraints of fronthaul delay, bandwidth limitation and different DU/CU resource capacity of MECs. All policies in DCUH are made with the objective of minimizing network energy consumption. To be specific, the heuristic is discussed in detail as follows.

To save the limited resources on edge MECs and reduce the energy consumption in RAN, we allocate UPFs on DC for the requests that can tolerate long-distance communication based on their end-to-end delay. Afterwards, in stage I, DCUH first finds out MEC2s and MEC3s that have to be activated because of fronthaul delay. Then it traverses the activated MEC2 or MEC3 to maximize their utilization and avoid awakening servers that would otherwise not be required. Unlike RFDH, DCUH allows distribution of acceptable servers for remaining

Algorithm 3: DU, CU & UPF Deployment Heuristic: Stage I

```

1: Collect the traffic information ( $l_q^s$ ,  $l_p^s$ ,  $T_s$  &  $c_s$ )
2: for All traffic  $s$  do
3:   if  $u$  is MEC2/3 & no other server accept  $l_p^s$  then
4:     Deploy UPF on  $u$ ,  $G_u^\eta - c_s$ 
5:     Add  $u$  into pre-activated MEC list  $\mathcal{G}_1$ 
6:   end if
7: end for
8: for rest traffic  $s$ , MEC2 or MEC3  $u$  in  $\mathcal{G}_1$  do
9:   if  $s$  from  $u$  then
10:    Deploy UPF on  $u$  for  $s$ ,  $G_u^\eta - c_s$ 
11:   else
12:     Based on  $l_p^s$ , append  $s$  to ' $u$ ' in dictionary  $\mathcal{S}_0$ 
13:   end if
14: end for
15: Sort MEC2/3 in  $\mathcal{G}_1$ , The more requests a MEC can serve, the higher the ranking.
16: Sort requests in Values in  $\mathcal{S}_0$ . The more MECs a request can access, the more backward.
17: for preactivated MEC2/3  $u$  in  $\mathcal{G}_1$ , Sorted traffic  $s$  in  $\mathcal{S}_0[u']$  do
18:   if Rest  $G_u^\eta > c_s$  then
19:     Deploy MEC on  $u$  for  $s$ ,  $G_u^\eta - c_s$ 
20:   end if
21: end for
22: for rest traffic  $s$  without UPF, unactivated MEC2/3 do
23:   Based on  $l_p^s$ , Append  $s$  to ' $u$ ' in dictionary  $\mathcal{S}_1$ 
24: end for
25: for MEC2/3  $u$  in  $\mathcal{S}_1$ , rest traffic  $s$  without UPF do
26:   Append  $s$  to ' $u$ ' in dictionary  $\mathcal{S}_2$ 
27: end for
28: Sort Keys in  $\mathcal{S}_1$ . The more requests a MEC can serve, the higher the ranking. Save sorted list in  $\mathcal{G}_2$ 
29: for MEC2/3  $u$  in  $\mathcal{G}_2$  do
30:   if  $u$  is MEC3 and  $\sum_s \mathcal{S}_2[u'] c_s \geq G_u^\eta$  of MEC2 then
31:     Replace it in the first place
32:   end if
33: end for
34: Sort requests in Values in  $\mathcal{S}_2$ . The more MECs a request can access, the more backward.
35: for MEC2/3  $u$  in  $\mathcal{G}$ , traffic in  $\mathcal{S}_2[u']$  do
36:   if  $s$  from  $u$  then
37:     Replace it in the first place in  $\mathcal{S}_2[u']$ 
38:   end if
39: end for
40: Repeat line 17-21 for  $\mathcal{G}_2$  and  $\mathcal{S}_2$ 
41: Append new activated MEC2/3 into  $\mathcal{G}_1$ 

```

unserved requests. The one accessed by more traffic will be set a higher priority to host the UPF. In addition, another principle defined to avoid activating multiple unnecessary MEC2s is to select MEC3 when the requested PU resource is bigger than its upper limit. At the end of stage I, based on the sources and destinations, DCUH applies DFS and end-to-end delay to filter paths that satisfy the condition.

In stage II, similar to the deployment of UPF, DCUH checks the availability of all activated MECs that have been activated so far. Subsequently, it sorts the applicable suspended MECs for the requests without DU based on how much traffic can access them. A higher priority of activation is assigned to the MECs which can support more traffic. Distributing DU from these sorted MECs is subjected to more limitations compared to UPF, which includes fronthaul delay, DU resources, bandwidth capacity and optional routing space decided in stage I.

Algorithm 3: DU, CU & UPF Deployment Heuristic: Stage II

```

1: Find paths from origins to corresponding destinations based on
    $l_p^s$ , store into dictionary  $D_0$ 
2: for activated MEC2 or MEC3  $u$  in  $\mathcal{G}_1$  do
3:   Deploy DU/CU for traffic  $s'$  from  $u$ 
4:    $G_u^e - T_s, G_u^s - \psi T_s$ 
5: end for
6: for preactivated MEC1  $u$  in  $\mathcal{G}_1$  do
7:   Deploy DU for traffic  $s$  from  $u$ 
8:    $G_u^e - T_s$ 
9: end for
10: for rest traffic  $s$  without DU do
11:   Based on  $l_q^s$  and  $D_0$ , append acceptable MECs and paths
      from ' $s$ ' to destinations in dictionary  $S_3$ 
12: end for
13: for Traffic  $s$  in Key list of  $S_3$  do
14:   Sorting its paths based on the hops
15: end for
16: for rest traffic  $s$  in Key list of  $S_3$  without DU do
17:   for all activated MEC1/2/3  $u$  in  $\mathcal{G}_1$  do
18:     for path in  $S_3[s']$  do
19:       if left  $G_u^e \geq T_s$  &
          bandwidth of each hop on the path before  $u \geq T_s$ 
          & bandwidth of each hop after DU  $\geq \psi T_s$  then
20:         Deploy DU on  $u$  for  $s, G_u^e - T_s$ 
21:         Store the used paths into dictionary  $D_1$ 
22:       end if
23:     end for
24:   end for
25: end for
26: for rest traffic  $s$  without DU, unactivated MEC1/2/3  $u$  do
27:   Based on  $l_q^s$ , append  $s$  to ' $u$ ' in dictionary  $S_4$ 
28: end for
29: Sort Keys in  $S_4$ . MEC1 first, then MEC2/3. The more requests
   a MEC can serve, the higher the ranking. Save sorted list in  $\mathcal{G}_3$ 
30: Repeat line 16-25 for  $\mathcal{G}_3, S_4$ 
31: for traffic  $s$  and its working path  $\omega$  in  $D_1$  do
32:   if  $u'$  on  $\omega$  in  $\mathcal{G}_1$  and  $G_{u'}^s \geq \psi T_s$  then
33:     deploy CU for  $s$  on  $u'$ 
34:      $G_{u'}^s - \psi T_s$ 
35:   else
36:     deploy CU for  $s$  on its destination  $u''$ 
37:      $G_{u''}^s - \psi T_s$ 
38:   end if
39: end for
    
```

Afterward, with the selected DUs, sources and destinations, routing paths are determined based on the minimum number of hops to save the switching energy costs. In the end, CU is preferentially deployed on the selected path to utilize the activated MECs.

For ease of understanding, we demonstrate these two stages by a simple example as shown in Figure 6. We assume nodes 2, 4, 8 receive requests from their respective coverage area, and the summation of their PU resource requirements is less than the MEC2 PU upper limit. None of the servers is pre-activated. To deploy baseband SFCs for these requests, in the first stage as shown in Figure 6(a), DCUH finds out the acceptable coverage of all the requests for UPF based on their end-to-end latency requirements. The UPF acceptable coverage areas of nodes 2, 4, 8 are represented by blue, green and red dash lines, respectively. Since only MEC2 and MEC3 can provide UPF, node 2 can get UPF service from nodes 3, 5. Nodes

4, 8 can get UPF service from nodes 3, 5, 9. Based on the assumption of their PU resource requirements, only node 3 requires activation in the first stage.

In Figure 6(b), dashed lines in 6(b) now represent the fronthaul delay limited acceptable coverage areas for DU service. As can be seen in Figure 6(b), since traffic from node 2 can not accept any other MEC except itself, this Node has to be activated to provide DU for its local requests. Consequently, to maximize the resource utilization of activated Node 3, a DU function will be placed on it to serve requests from node 2 and 4. For the remaining requests on node 8, although they can accept the DU service from node 5, 8, 9, DCUH will activate node 8 as it is MEC1 and it has the minimum activation cost among these three. In the end, CU for three requests is placed on node 3 and the selected working path is marked in red.

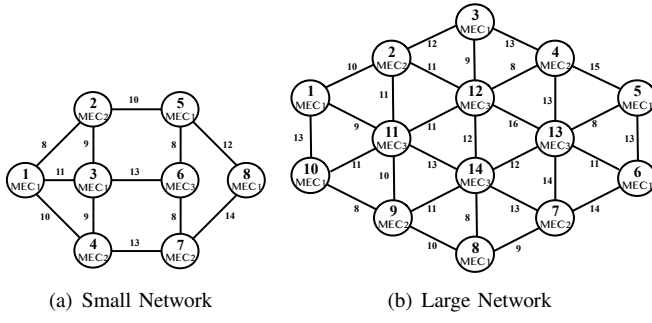
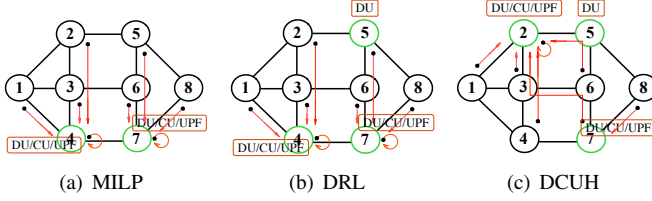
B. Time complexity

The complexity of the DCUH is calculated as follows. In stage I, in the context of C MEC2/3s, J pre-activated MEC2/3s and m pre-activated MEC1s, the complexity of deploying UPF for requests on these pre-activated MECs is $O(2NJ + J\log J + N\log N - J^2)$. Under the assumption that J requests get UPF from their local MECs, the complexity of providing UPF for the rest $N - P$ requests can be represented by $O((N - J)^2 + 3(C - J)(N - J) + (C - J) + (N - J)\log(N - J))$. Furthermore, to statisticize the distance and hops of all the paths from every source to its destination that fit the end-to-end delay, we applied the DFS with the time complexity of $O(N^2 + NE)$. In stage II, the complexity of utilizing P activated MECs can be represented by $O(2N + (N - J - m)S_2\log S_2 + (N - J - m)(J + m)S_2)$, where m is the number of pre-activated MEC1, S_2 represents the average length of Values in dictionary S_2 , and $(N - J - m)$ is the rest of the traffic without DU. If there are only $(J + m)$ requests that have got service from these activated MECs, there are still $(N - J - m)$ that need to find DU service from $(N - J - m)$ MECs. Therefore, the complexity of this process is $(N - J - m)^2(S_3 + S_4)$, where S_3, S_4 are the average length of Values in dictionary S_3 and S_4 , respectively. The complexity for CU placement in the end can be written as $O(ND_1)$ and D_1 is the average length of Values in dictionary D_1 .

Overall, the time complexity of DCUH can be represented by $O((N - J)^2 + 3(C - J)(N - J) + (C - J) + (N - J)\log(N - J) + N^2 + NE + 2N + (N - J - m)S_2\log S_2 + (N - J - m)(J + m)S_2 + (N - J - m)^2(S_3 + S_4) + ND_1)$. Instead of applying math solvers which iterate over the solving space and sacrifice training and communication overhead of machine learning solutions, DCUH can highly decrease the reaction time and improve feasibility in real networks.

VI. SIMULATION RESULTS

In this section, we provide the setup information of Open RAN components and DRL-based algorithms. Restricted by the scalability of MILP, firstly we compare the energy-saving performance of proposed algorithms in a small network consisted of 8 MECs. After that, their performance in a 14-node, 29-link network is further explored. To demonstrate the


Fig. 7: Simulation Networks.

Fig. 8: Baseband Function Placement and Path Provisioning of DRL and DCUH Algorithms for traffic F .

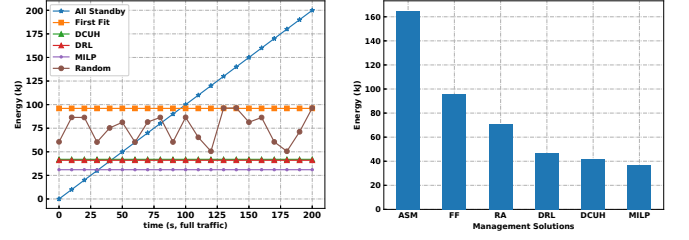
training cost of DRL-based algorithms, we calculate their time and space complexity.

A. Simulation Setup

The simulated MEC networks with 8 and 14 servers are shown in Figures 7(a) and 7(b). The DU and CU capacity of all MECs are set to 50 Gbits/s. The PU resource of MEC2 and MEC3 are set to 32 cores and 50 cores. Bandwidth of each link is 50 Gbit/s. The power of MEC1, MEC2 and MEC3 are set to 100W, 170W and 200W, respectively. Their corresponding activation power and time cost are set to 500W and 20s, 600W and 25s, 700W and 30s. The switching energy consumption on each node is unified to 0.5kJ. For each set of requests received by a MEC server, the data size, PU resource requirements are randomly distributed between 8 Gbits/s to 12 Gbits/s and 3 cores to 5 cores. The fronthaul delay is set between 11 km to 21 km, and the end-to-end delay is set between 28 km to 43 km. In addition, we use 0.2 as the traffic decreasing ratio ψ after it is processed by DU. In the DRL part, the batch size of MADDPG is set to 200. The learning rate μ is set to 10^{-4} . The target network update coefficient τ of MADDPG and the reward discount γ are set to 0.1 and 0.05, respectively.

B. 8-MEC network

To demonstrate the effectiveness of our designed algorithms, we first provide the location of activated MECs, provisioned functions and routing paths for a traffic set F as shown in Figure 8. 8 requests in F consist of fronthaul delay [14, 20, 17, 19, 19, 17, 17, 17] united in km, end-to-end delay [28, 38, 40, 29, 41, 32, 34, 42] united in km, data size [11, 9, 10, 9, 9, 8, 10, 11] united in Gbits/s and computing resource requirement [5, 5, 5, 5, 4, 3, 5, 4] united in cores. Activated MECs and routing paths are marked by green circles and red arrows, respectively.

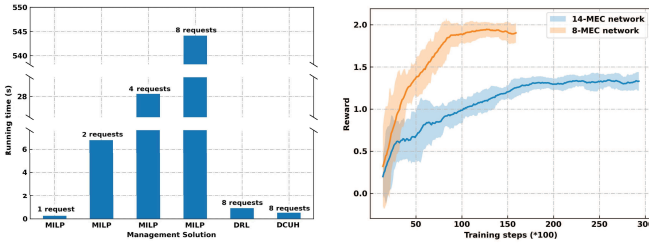

Fig. 9: Energy Consumption Comparison Between Different Joint Baseband Function Deployment Algorithms

In addition, we compare the energy consumption of F under several management policies with the increase in network idle time as shown in Figure 9(a). Blue, orange, gray, purple, red and green lines represent the requests of all standby mode (ASM), first fit (FF) [40], random allocation (RA), MILP, DRL and DCUH, respectively. Among them, without activation cost, ASM keeps all MECs awake in spite of the request status. FF is to select the first available server while traversing the resources. RA randomly selects the resources on the premise of fulfilling all the requests. ASM is the most energy efficient solution in the beginning, whereas it becomes the worst when the idle time exceeds 100s. This observation illustrates the energy-saving benefit of hibernating the MEC when their idle time is long. The results of MILP are considered as a benchmark according to its characteristics. Among rest strategies, DCUH and the DRL-based strategy acquire similar energy saving performance and stand out most prominently. To get generalized performance comparison, in Figure 9(b), we summarize the energy consumption of these solutions for 50 random requests with 150s of network vacant time. DCUH and the DRL-based solution can save more than 45% energy compared to FF. It is worth noticing that although RA can acquire better performance than FF, its results are obtained in the promise of satisfying all the requests whereas it can not be assured in practical applications.

Figure 10(a) shows the running time of our proposed solutions with different amounts of traffic requirements by utilizing a machine with 3.2GHz 6-core 8th-generation Intel Core i7. In the case of full traffic, MILP requires 544.3s to get the optimal result, therefore violating real-time response requirements in 5G services. In contrast, the less than 1s reasoning time of DCUH and DRL confirms their importance in practical applications.

C. 14-MEC network

To further explore the performance of the DRL-based solution and DCUH in a larger network, assuming Node 2 is pre-activated, we simulate the locations of all provisioned functions and routing paths for another traffic set T with 14 requests in network 7(b). MILP is not able to be solved in this network. Traffic set T consist of fronthaul delay [14, 20, 17, 19, 19, 17, 17, 17, 13, 15, 20, 18, 16, 11] united in km, end-to-end delay [28, 38, 40, 29, 41, 32, 34, 42, 37, 29, 28, 31, 28, 31] united in km, data size [11, 9, 8, 9, 9, 8, 10, 11] united in Gbits/s and computing resource requirement [5, 5, 5, 5, 4, 3, 5, 4] united in cores. Activated MECs and routing paths are marked by green circles and red arrows, respectively.



(a) Running Time of Different Management Solutions in the 8-MEC Network. (b) The Convergence Property of DRL Algorithms.

Fig. 10: Complexity comparison.

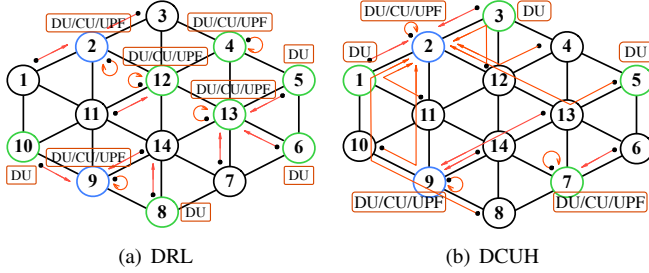


Fig. 11: Baseband Function Placement and Path Provisioning of DRL and DCUH Algorithms for traffic T .

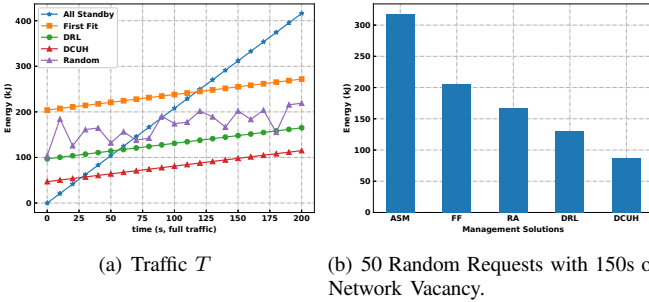


Fig. 12: Energy Consumption Comparison Between Different Joint Baseband Function Deployment Algorithms.

10, 11, 10, 9, 8, 10, 9, 9] united in Gbits/s and computing resource requirements [3, 4, 5, 5, 3, 3, 5, 5, 3, 3, 3, 3, 5, 3] united in cores. These results can be found in Figure 11, where the standby and new activated MECs are marked by blue and green circles. The Red arrows indicate selected routing paths. Consistent with the 8-MEC network, the energy consumption of T under various management policies versus network vacant time is also compared as shown in Figure 12(a). Because of maintenance costs of pre-activated nodes, the energy costs of all strategies increase as idle time. Otherwise, the energy costs of FF and DRL and DCUH will remain constant as they are in Figure 9(a).

Figure 12(b) demonstrates the energy cost of 50 groups of random requests with 150s of network vacant time. Similar to the performance in small networks, DCUH and DRL can achieve the best performance. However, as the network size increases, the relative benefits obtained by DRL gradually decrease. A possible explanation for this result is that due to the increase in the number of agents, the cooperative relationship between agents becomes more complex, which hurts the accuracy of the fitting.

D. DRL training cost

Here we analyze both the time and space complexity and execution cost of MADDPG in this subsection. Referring to [41], the time complexity of reinforcement learning is sub-linear in the length of the state period and can be represented by $O(\text{training steps})$. To demonstrate it, we summarize the convergence property of MADDPG in Figure 10(b). Yellow and blue lines represent convergence performance in the 8-MEC network with 2 agents and 14-MEC network with 3 agents, respectively. The advantage in converging speed and reward of DRL in the small network can be explained in part by its lower agent number and network complexity in terms of state and action spaces. In the small network, each agent is responsible for the activation management of 4 nodes, while in the large one, three agents are responsible for 5, 5 and 4 nodes, respectively. In addition, the space complexity is proved to be sub-linear in the size of state space, action space, and step numbers per episode. It can be written as $O(\sum_l^L \sum_q^Q F_s^{lq} F_a^{lq} F_h^{lq})$, where Q is the set of actor and critic, F_s is the number of states, F_a is the number of outputs, and F_h is the number of training steps in each episode. Based on these values aforementioned, the space complexities of MADDPG in small and large networks can be written as $O(2.84E5)$ and $O(1.21E6)$.

Overall, with acceptable complexity, DCUH and the DRL-based solution approach the effectiveness of MILP and help save energy consumption in baseband function deployments for Open RAN.

VII. FEASIBILITY EVALUATION OVER OPEN RAN TESTBED

To verify the effectiveness of our proposed algorithms on energy-saving performance, and draw on the framework in [42], [43], we build an Open RAN testbed by utilizing OpenDaylight, OpenStack, OSM and some other open source application programming interfaces (APIs). Furthermore, by measuring the power characteristic of MEC and network reaction delays, we explore the implementation feasibility of the designed algorithm within practical networks.

A. Testbed Orchestration

The Open RAN testbed deployment and its orchestration are shown in Figures 13 and 14. There are three MECs distributed at the University of Bristol (MEC-A, main), MShed museum (MEC-B) and We The Curious museum (MEC-C). Each of them consists of a server set and edge monitoring probs. To enable a flexible, programmable and agile network, based on OSM, OpenDaylight and OpenStack, we build an orchestrator, a virtualized infrastructure management (VIM) controller and a software-defined network (SDN) controller inside MEC-A to manage the network slices and RAN. In the testbed, the request characteristics, remaining resource information and activation status of each server are gathered by a central monitor through distributed monitoring probs at each edge. On the basis of this information, our algorithms decide the optimal MEC activation, function placement and routing provisioning instructions, which are then interpreted into assembly language by an

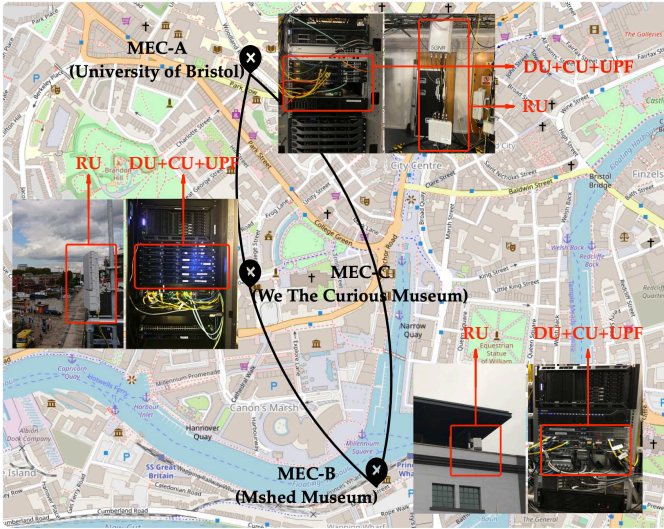


Fig. 13: Open RAN Testbed Urban Deployment in Bristol. The map image is taken from OpenStreetMap (<https://www.openstreetmap.org>).

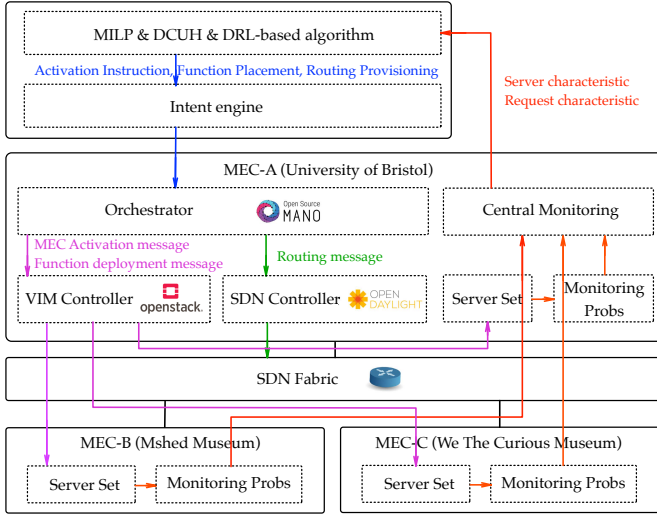


Fig. 14: Closed-loop Open RAN Testbed Orchestration.

intent engine (IE) [44]. By creating closed-loop automation that includes intent capture, intent translation and virtualized function activations, IE can continuously monitor and adjust to ensure service alignment with end-to-end requirements. SDN and VIM controllers are responsible for the execution of path provisioning and baseband function deployment, respectively.

B. Feasibility verification

In this subsection, as shown in Figure 15, we explain the deployment of baseband functions in our testbed according to IEEE communication and European Telecommunications Standards Institute (ETSI) Open RAN standards. A MEC server set consists of a top-of-rack switch (TOR) and few commercial-off-the-shelves (COTSs) and comprises network in-host switching and external connectivity. Specifically, in-host switching is achieved by Linux kernel packet switching and forwarding packages, and external connectivity is realized by the network interface controller (NIC) that connects to

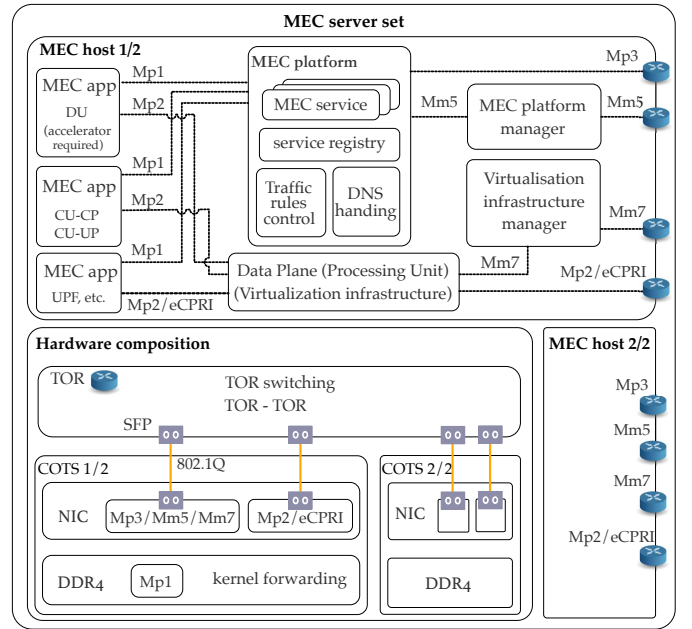


Fig. 15: Baseband Function Deployment Based on IEEE and ETSI Standards in a MEC server set. (Yellow lines denote wired transmission based on 802.1Q; Gray squares denote the SFP transceiver; Blue cylinders indicate network switching).

TOR via fiber with the help of small form-factor pluggable transceivers (SFPs). TOR can therefore realize TOR switching and TOR-TOR switching that happens inside rack and between MECs. Noting that all connections to the TOR marked in yellow lines are realized by fiber and IEEE 802.1Q protocols [45].

These physical devices are the basis of virtualized MEC host modules and interfaces. Referring to ETSI standards [46], Mp1 connects the MEC platform to MEC applications (MEC app). Mp2 manages the application routing between the data plane. DU, CU control plane (CU-CP), CU user plane (CU-UP) and UPF are implemented as MEC apps, therefore, Mp1 and Mp2 are two essential interfaces in the SFC that are responsible for the transmission between baseband functions. Mp3 is the bridge of communication between different MECs. Mm7 and Mm5 are the management interfaces that allow OSM to manage the hibernation, activation, or standby of the MEC apps. These interfaces and their connected MEC host modules are detailed in Figure 15. There are two physical interfaces on the NIC. One can be applied for data layer Mp3, Mm5, and Mm7. The other can be used as Mp2. eCPRI can be realized as a type of Mp2 data plane network connectivity. Additionally, the kernel forwarding function utilizing non-uniform memory access (NUMA) on the installed DDR4 memory modules can be seen as Mp1. In the end, the switches connected by MmX and MpX interfaces on the right of the MEC host illustrate that all the external communications between MEC hosts must go through the TOR.

Moreover, to reflect the importance of activation cost in determining the effectiveness of baseband function deployment algorithms, we test the activation time and corresponding power, CPU temperature and system temperature changes of MEC-A during startup, cold reboot and warm reboot process.

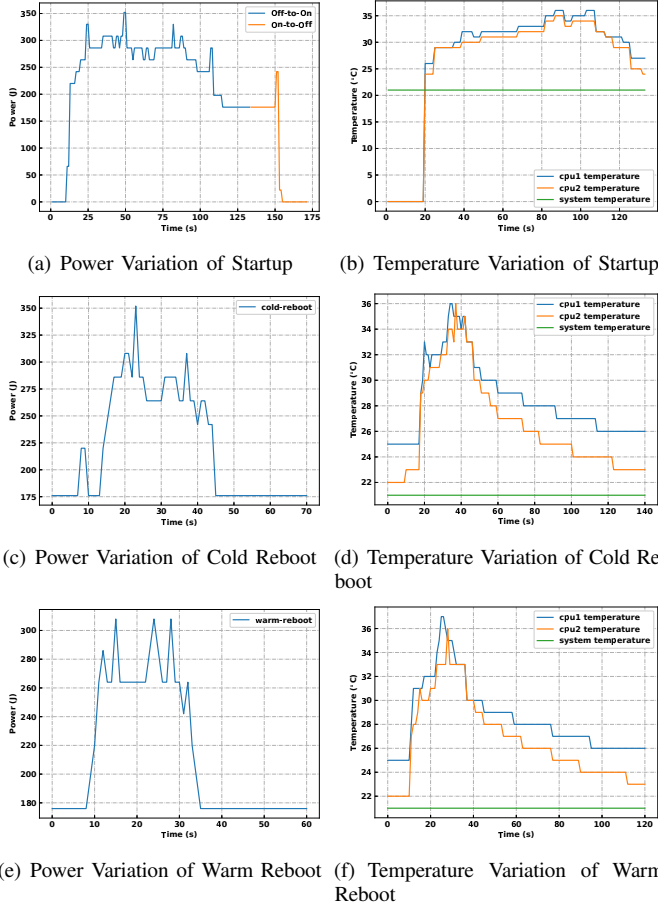


Fig. 16: Power and Temperature Variation During Three Types of Server Activation.

This server has 2 CPUs, each with 14 cores and 2 threads per core. A startup is to wake up the server from the shutdown state. A cold boot resets running hardware and reloads the operating system. Warm boot, on the other hand, is to regain the initial state of a server without hampering the power source. As shown in Figure 16, MEC will experience a manifest power surge for a period of time and return to a stable state in either case. Unlike the power that drops rapidly after activation, CPU temperature will take longer to cool down and approximate to the system temperature. In addition, it is found that the higher the dormancy degree of the server, the longer the activation time and the higher the activation power. Activation energies for startup, cold and warm reboots are around 26.9kJ, 8.1kJ and 7.1kJ, respectively. Contrary to expectations, there is a momentary power surge in the shutdown process.

We also perform a server stress test that monitors the trend of power cost, CPU temperature and system temperature with increasing load after a MEC is activated. The results, as shown in Figure 17, indicate that the tested server characteristics and traffic load are roughly governed by a linear relationship. It is worth noting that the highest CPU temperature goes to 60 degrees when fully loaded. In the deployment of Open RAN and management of MEC network resources, since distributed edge servers do not have complete supporting equipment such as air conditioners compared to data centers,

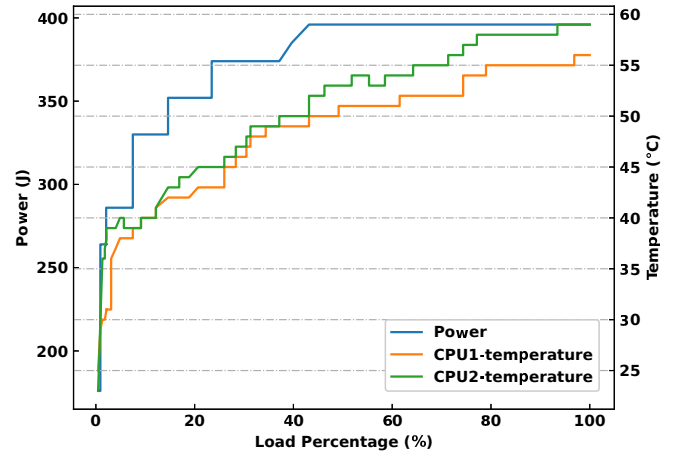


Fig. 17: Power and Temperature Characteristics Load Stress Test.

the performance of MEC hardware components affected by load should also be taken into account. In the end, we test that the transmission delay of control message from MEC-A to MEC-B and MEC-C is less than 10ms. These results prove the feasibility of management algorithms in real networks and serve as a base for future studies in designing more practical baseband function deployment strategies.

VIII. CONCLUSION

This paper has argued that the emerging Open RAN architecture and time-space usage dynamics have placed a severe burden on the management of baseband function deployment regarding the network energy-saving efficiency. Current strategies fail to considerate multiple UPFs and the activation time costs, therefore they are not able to fulfill 5G diverse traffic and could lead to unnecessary energy waste. In this paper, we proposed a scenario that divides the radio access network into clusters with three types of MEC servers. DU, CU and UPF are able to be deployed on the same or different hosts. With the purpose of minimizing the energy cost in RAN while subjecting to the network resources and latency constraints, we design a MILP formulation, a multi-agent DRL-based algorithm and a heuristic and prototype an Open RAN testbed in Bristol to verify the feasibility of these proposed algorithms. Simulation results show that DCUH and the DRL-based solution can approach the benchmark of MILP and gain great improvements compared to FF and other methods.

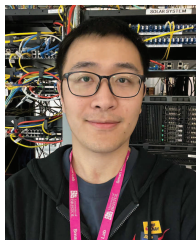
ACKNOWLEDGMENTS

The authors would like to express their thanks for support from the China Scholarship Council, European Commission's Horizon 2020 research and innovation program under grant agreement No 871428, 5G-CLARITY project and 5G Logistics project funded by the Department for Digital, Culture, Media and Sport, U.K.

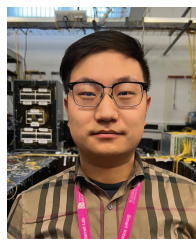
REFERENCES

- [1] S. K. Singh, R. Singh, and B. Kumbhani, "The evolution of radio access network towards open-ran: Challenges and opportunities," in *2020 IEEE Wireless Communications and Networking Conference Workshops (WCNCW)*. IEEE, 2020, pp. 1–6.

- [2] A. S. Abdalla, P. S. Upadhyaya, V. K. Shah, and V. Marojevic, "Toward next generation open radio access networks—what o-ran can and cannot do!" *IEEE Network*, 2022.
- [3] H. Tataria, M. Shafi, A. F. Molisch, M. Dohler, H. Sjöland, and F. Tufvesson, "6g wireless systems: Vision, requirements, challenges, insights, and opportunities," *Proceedings of the IEEE*, vol. 109, no. 7, pp. 1166–1199, 2021.
- [4] R. Joda, T. Pamuklu, P. E. Iturria-Rivera, and M. Erol-Kantarci, "Deep reinforcement learning-based joint user association and cu-du placement in o-ran," *IEEE Transactions on Network and Service Management*, 2022.
- [5] S. D'Oro, L. Bonati, F. Restuccia, M. Polese, M. Zorzi, and T. Melodia, "SI-edge: Network slicing at the edge," in *Proceedings of the Twenty-First International Symposium on Theory, Algorithmic Foundations, and Protocol Design for Mobile Networks and Mobile Computing*, 2020, pp. 1–10.
- [6] F. Dressler, C. F. Chiasserini, F. H. Fitzek, H. Karl, R. L. Cigno, A. Capone, C. Casetti, F. Malandrino, V. Mancuso, F. Klingler et al., "V-edge: Virtual edge computing as an enabler for novel microservices and cooperative computing," *IEEE Network*, vol. 36, no. 3, pp. 24–31, 2022.
- [7] B. Balasubramanian, E. S. Daniels, M. Hiltunen, R. Jana, K. Joshi, R. Sivaraj, T. X. Tran, and C. Wang, "Ric: A ran intelligent controller platform for ai-enabled cellular networks," *IEEE Internet Computing*, vol. 25, no. 2, pp. 7–17, 2021.
- [8] E. Tranos and P. Nijkamp, "Mobile phone usage in complex urban systems: a space-time, aggregated human activity study," *Journal of Geographical Systems*, vol. 17, no. 2, pp. 157–185, 2015.
- [9] A. Lacava, M. Polese, R. Sivaraj, R. Soundrarajan, B. S. Bhati, T. Singh, T. Zugno, F. Cuomo, and T. Melodia, "Programmable and customized intelligence for traffic steering in 5g networks using open ran architectures," *arXiv preprint arXiv:2209.14171*, 2022.
- [10] H. Li, K. Assis, A. Vafeas, S. Yan, and D. Simeonidou, "Resilient and energy efficient du-cu-mec deployments for service oriented reliable next generation metro access network," in *47th WWRf*, 2022.
- [11] R. I. Tinini, L. C. Reis, D. M. Batista, G. B. Figueiredo, M. Tornatore, and B. Mukherjee, "Optimal placement of virtualized bbu processing in hybrid cloud-fog ran over twdm-pm," in *GLOBECOM 2017-2017 IEEE Global Communications Conference*, IEEE, 2017, pp. 1–6.
- [12] R. Mijumbi, J. Serrat, J.-L. Gorricho, J. Rubio-Loyola, and S. Davy, "Server placement and assignment in virtualized radio access networks," in *2015 11th international conference on network and service management (CNSM)*, IEEE, 2015, pp. 398–401.
- [13] Z. Gao, S. Yan, J. Zhang, B. Han, Y. Wang, Y. Xiao, D. Simeonidou, and Y. Ji, "Deep reinforcement learning-based policy for baseband function placement and routing of ran in 5g and beyond," *Journal of Lightwave Technology*, vol. 40, no. 2, pp. 470–480, 2021.
- [14] T. Sigwele, Y. F. Hu, and M. Susanto, "Energy-efficient 5g cloud ran with virtual bbu server consolidation and base station sleeping," *Computer Networks*, vol. 177, p. 107302, 2020.
- [15] Anritsu, "eCPRI Transport White Paper," Tech. Rep. 1914.3 (RoE), 2018. [Online]. Available: <https://dl.cdn-anritsu.com/en-en/test-measurement/files/Technical-Notes/White-Paper/m1900a-ecpri-err100.pdf>
- [16] R. Li, R. Wang, N. Halachmi, Q. Zhong, W. Cheng, L. Wang, and J. Wang, "X-ethernet: Enabling integrated fronthaul/backhaul architecture in 5g networks," in *2017 IEEE Conference on Standards for Communications and Networking (CSCN)*, IEEE, 2017, pp. 121–125.
- [17] S. Niknam, A. Roy, H. S. Dhillon, S. Singh, R. Banerji, J. H. Reed, N. Saxena, and S. Yoon, "Intelligent o-ran for beyond 5g and 6g wireless networks," *arXiv preprint arXiv:2005.08374*, 2020.
- [18] Y. Xiao, J. Zhang, Z. Gao, and Y. Ji, "Service-oriented du-cu placement using reinforcement learning in 5g/b5g converged wireless-optical networks," in *Optical Fiber Communication Conference*, Optical Society of America, 2020, pp. T4D–5.
- [19] L. M. M. Zorello, M. Sodano, S. Troia, and G. Maier, "Power-efficient baseband-function placement in latency-constrained 5g metro access," *IEEE Transactions on Green Communications and Networking*, 2022.
- [20] Xiao, Yuming and Zhang, Jiawei and Ji, Yuefeng, "Energy-efficient du-cu deployment and lightpath provisioning for service-oriented 5g metro access/aggregation networks," *Journal of Lightwave Technology*, vol. 39, no. 17, pp. 5347–5361, 2021.
- [21] J. Medved, R. Varga, A. Tkacik, and K. Gray, "Opendaylight: Towards a model-driven sdn controller architecture," in *Proceeding of IEEE International Symposium on a World of Wireless, Mobile and Multimedia Networks 2014*, IEEE, 2014, pp. 1–6.
- [22] O. Sefraoui, M. Aissaoui, M. Eleuldj et al., "Openstack: toward an open-source solution for cloud computing," *International Journal of Computer Applications*, vol. 55, no. 3, pp. 38–42, 2012.
- [23] A. M. et al., "A white paper prepared by the osm end user advisory group," ETSI, France, Tech. Rep., 2021. [Online]. Available: <https://vetstudies.edu/donteatthosefries.html>
- [24] 3GPP, "Technical specification group radio access network; study on new radio access technology, radio access architecture and interfaces," TR 38.801, Rel.14, April 2017.
- [25] A. De la Oliva, J. A. Hernandez, D. Larrabeiti, and A. Azcorra, "An overview of the cpri specification and its application to c-ran-based lte scenarios," *IEEE Communications Magazine*, vol. 54, no. 2, pp. 152–159, 2016.
- [26] Z. Zhou, M. Dong, K. Ota, G. Wang, and L. T. Yang, "Energy-efficient resource allocation for d2d communications underlying cloud-ran-based lte-a networks," *IEEE Internet of Things Journal*, vol. 3, no. 3, pp. 428–438, 2015.
- [27] L. Bonati, M. Polese, S. D'Oro, S. Basagni, and T. Melodia, "Open, programmable, and virtualized 5g networks: State-of-the-art and the road ahead," *Computer Networks*, vol. 182, p. 107516, 2020.
- [28] L. Bonati, S. D'Oro, M. Polese, S. Basagni, and T. Melodia, "Intelligence and learning in o-ran for data-driven nextg cellular networks," *IEEE Communications Magazine*, vol. 59, no. 10, pp. 21–27, 2021.
- [29] S. Mollahasani, M. Erol-Kantarci, and R. Wilson, "Dynamic cu-du selection for resource allocation in o-ran using actor-critic learning," in *2021 IEEE Global Communications Conference (GLOBECOM)*, IEEE, 2021, pp. 1–6.
- [30] Z. Allybokus, N. Perrot, J. Leguay, L. Maggi, and E. Gourdin, "Virtual function placement for service chaining with partial orders and anti-affinity rules," *Networks*, vol. 71, no. 2, pp. 97–106, 2018.
- [31] J. Bisschop, *AIMMS optimization modeling*. Lulu.com, 2006.
- [32] K. Assis, S. Peng, R. Almeida, H. Waldman, A. Hammad, A. Santos, and D. Simeonidou, "Network virtualization over elastic optical networks with different protection schemes," *Journal of Optical Communications and Networking*, vol. 8, no. 4, pp. 272–281, 2016.
- [33] C. C. Bennett and K. Hauser, "Artificial intelligence framework for simulating clinical decision-making: A markov decision process approach," *Artificial intelligence in medicine*, vol. 57, no. 1, pp. 9–19, 2013.
- [34] D. Silver, G. Lever, N. Heess, T. Degris, D. Wierstra, and M. Riedmiller, "Deterministic policy gradient algorithms," in *International conference on machine learning*. PMLR, 2014, pp. 387–395.
- [35] R. Lowe, Y. I. Wu, A. Tamar, J. Harb, O. Pieter Abbeel, and I. Mordatch, "Multi-agent actor-critic for mixed cooperative-competitive environments," *Advances in neural information processing systems*, vol. 30, 2017.
- [36] V. Mnih, K. Kavukcuoglu, D. Silver, A. Graves, I. Antonoglou, D. Wierstra, and M. Riedmiller, "Playing atari with deep reinforcement learning," *arXiv preprint arXiv:1312.5602*, 2013.
- [37] K. M. Chandy, "Parallel program design," in *Opportunities and Constraints of Parallel Computing*. Springer, 1989, pp. 21–24.
- [38] R. Tarjan, "Depth-first search and linear graph algorithms," *SIAM journal on computing*, vol. 1, no. 2, pp. 146–160, 1972.
- [39] R. Cole, "Parallel merge sort," *SIAM Journal on Computing*, vol. 17, no. 4, pp. 770–785, 1988.
- [40] B. S. Baker, "A new proof for the first-fit decreasing bin-packing algorithm," *Journal of Algorithms*, vol. 6, no. 1, pp. 49–70, 1985.
- [41] J. Leem and H. Y. Kim, "Action-specialized expert ensemble trading system with extended discrete action space using deep reinforcement learning," *Plos one*, vol. 15, no. 7, p. e0236178, 2020.
- [42] S. Fdida, N. Makris, T. Korakis, R. Bruno, A. Passarella, P. Andreou, B. Belter, C. Crettaz, W. Dabbous, Y. Demchenko et al., "Slices, a scientific instrument for the networking community," *Computer Communications*, vol. 193, pp. 189–203, 2022.
- [43] E. Amin, V. Constantinos, T. Stavros, B. Klodian, F. Hamid, N. Reza, and S. Dimitra, "Smart internet lab's testbed as a platform for research & innovation," in *47th WWRf*, 2022.
- [44] 5G-CLARITY, "Intent based slice management demonstration," accessed: July. 4, 2022. [Online]. Available: <https://www.youtube.com/watch?v=5Jsc2ds-etI>
- [45] "IEEE Standard for Local and Metropolitan Area Networks—Bridges and Bridged Networks," *IEEE Std. 802.1Q*, 2018.
- [46] M. ETSI, "Mobile edge computing (mec); framework and reference architecture," *ETSI, DGS MEC*, vol. 3, pp. 1–18, 2016.



Haiyuan Li received his B.Sc degree in communication engineering from Central South University, China, in 2019, and his M.Sc degree in communication networks and signal processing from the University of Bristol, U.K., in 2020. He is currently pursuing his Ph.D. degree with the school of electrical and electronic engineering at the University of Bristol. His research interests include Mobile Edge Computing, Deep Reinforcement Learning, Parallel Computing, Game Theory, Beyond 5G and Network Optimization.



Ruizhi Yang received his B.Sc degree in applied physics (basic science of communication) from Beijing University of Posts and Telecommunications, China, in 2016, and M.Sc degree in optical communications and signal processing from the University of Bristol, U.K., in 2019. He is currently pursuing his Ph.D. degree with the department of electrical and electronic engineering at the University of Bristol. His research interests include Programmable ROADM, Multi-core Fiber in Optical Networks, Topology Optimization in SDM/WDM-based Optical Networks. Quality of Transmission Prediction and Machine learning in Optical Networks.



Amin Emami is a researcher at the Smart Internet Lab with the University of Bristol, he is also a senior member of the 5GUK testbed team which is one of the most advanced 5G and beyond testbeds in the UK. He received his M.Sc. degree in Electrical and Electronics Engineering from the University of Najafabad, Iran, in 2011. His strong technical and practical skills, as well as interpersonal skills, enable him to work with and direct contribution to a wide range of European and UK national projects such as 5GCLARITY, 5GVICTORI, 5GPICTURE, 5GASP,

MetroHaul as well as UK DCMS funded project 5G Smart Tourism. He is a competent IT professional with a proven track record in networking, cloud computing, and virtualisation offering 18 years of both academic and industrial experience. His research interests lie in the areas of 5G core and RAN/ORAN, cloud computing, SDN, NFV, MANO, and their applications toward 5G networks.

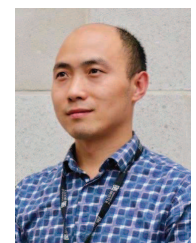


Reza Nejabati is currently a chair professor of intelligent networks and head of the High-Performance Network Group in the Department of Electrical and Electronic Engineering in the University of Bristol, UK. He is also a visiting professor and Cisco chair in the Cisco centre for Intent Based Networking in the Curtin University, Australia. He has established successful and internationally recognised experimental research activities in “Autonomous and Quantum Networks”. Building on his research, He co-founded a successful start-up company (Zeetta Networks Ltd) with 25 employees and £6m funding.



Karcus Day R. Assis received his B.Sc. degree in electrical engineering from the Federal University of Paraíba (currently Federal University of Campina Grande) in 1998, his M.Sc. degree from the Federal University of Espírito Santo in 2000, and his Ph.D. degree in electrical engineering from the University of Campinas in 2004. From 2004 to 2010, he was with Salvador University, Federal University of ABC-UFABC and Federal University of Recôncavo da Bahia, Brazil. In 2010, he joined the Department of Electrical and Computer Engineering, Federal

University of Bahia, Salvador, Brazil, where he is an Associate Professor. Currently, Karcus has returned to the High Performance Networks Group, Smart Internet Lab at the University of Bristol, U.K., as a visiting researcher, having held this position in 2015. His research interests include Optical Networking, Traffic Engineering, Resource Management, Network Survivability, Machine Learning, Future Internet, and Telecommunication Networks Optimization and Projects. He won an International Visiting Fellowship in 2017 and spent some time at Essex University, United Kingdom.



Shuangyi Yan is a Senior Lecturer in the High Performance Networks Group in the Smart Internet Lab at the University of Bristol. He received his B.E degree in information engineering from Tianjin University, Tianjin, China in 2004. In 2009, he received his PhD degree in Optical Engineering from Xi'an Institute of Optics and Precision Mechanics, CAS, Xi'an, China. From 2011 to 2013, Dr Yan worked at Hong Kong Polytechnic University, Hong Kong, as a postdoctoral researcher, investigating spectrally-efficient long-haul optical transmission systems and low-cost short-range transmission systems. In July 2013, he joined the University of Bristol. His research focuses on machine-learning applications in dynamic optical networks and 5G Beyond networks, programmable optical networks, and data centre networks.



Antonis Vefas is a Senior Research Associate in 5G Network Systems Engineering & Administration at the University of Bristol. He received his B.E degree from the University of Bristol, U.K. in 2014. In 2019, he received his PhD degree in Electrical and Electronic Engineering from the University of Bristol, U.K. He specialises in multimodal sensing, wireless networking and embedded hardware.



Dimitra Simeonidou (FREng, FIEEE) is a Full Professor at the University of Bristol, the CoDirector of the Bristol Digital Futures Institute, and Director of the Smart Internet Lab. Her research focuses on the fields of high performance networks, programmable networks, wireless-optical convergence, 5G/B5G and smart city infrastructures. She is increasingly working with Social Sciences on topics of digital transformation for society and businesses. Dimitra has also been the Technical Architect and the CTO of the Smart City project Bristol Is Open. She is currently leading the Bristol City/Region 5G urban pilots. She is the author and co-author of over 500 publications, numerous patents and several major contributions to standards. Dimitra is a Fellow of the Royal Academy of Engineering, a Fellow of the Institute of Electrical and Electronic Engineers, and a Royal Society Wolfson Scholar.